Functional Materials 12, No.4 (2005)

Emission of nanoparticles at the crack front during cleavage of alkali-halide single crystals

I.A.Massalimov, I.A.Madyukov[*], *V.S.Shevchenko*[*], *F.Kh.Urakaev*[*]

Scientific & Research Institute of Low Tonnage Chemicals and Reagents, RF Ministry of Education, 450029 Ufa, Russian Federation
[*]Institute for Mineralogy and Petrography, Siberian Branch of Russian Academy of Sciences, 630090 Novosibirsk, Russian Federation

Equations of statistical physics are applied to numerical aspects of energy balance at the crack front with reference to the cleavage of alkali halide single crystals. The possibility of nanoparticles emission during the dynamic failure is ascertained theoretically.

Уравнения статистической физики применены к численным аспектам энергетического баланса у фронта трещины для случая раскалывания щелочно-галоидных монокристаллов. Теоретически оценена вероятность образования наночастиц в процессе динамического разрушения.

In the description of a crack evolution, we used the concept of the pre-failure zone presented in [1–3]. This zone covers a large group of atomic bonds within the bulk of a material at the crack tip. During mechanical action upon brittle solids [4–6], the strained fields arise at structural heterogeneities and deformations, where non-linear features of atomic interactions become apparent and a high rupture possibility of strained bonds appears. Linear dimension of such a field is estimated to be $\delta \sim 10^{-6}$ to 10^{-3} cm, according to [1–4, 6]. The transience of either fracturing or impact hinders their detailed study, and only the phenomena of fractoemission (FE) [7] can provide more information. FE includes the emission of photons and electrons [8], volatile products of mechanical failure and the material structure components in the atomic, ionic, molecular, fractal form [7–12], and small particles [13]. In the present work, we studied the possibility of nanoparticle emission from the crack front during failure of alkali halide crystals (AHC) along the cleavage plane (100).

During propagation of a crack, the energy E^* is released at its front area δ. This energy is the difference between the accumulated energy E_c and the energies of [14]: elastic state relaxation E_e, total energies of new surface formation and plastic strain $E_s + E_d$ [15, 16], kinetic energies of the fracture fragments E_k [14, 15], and the FE energy E_f, i.e., the sum of athermic and thermic constituents $E_f = E_a + E_t$ [8, 11, 12]. The elastic energy E_e disappears in the strained areas when a crack appears. Hence, the energy balance at the crack front presented in [14] can be rewritten as:

$$E^* = E_c - E_e = E_s + E_d + E_k + E_f. \qquad (1)$$

The left part of equation (1), being presented as $E_c - E_e$, emphasizes the fact that not the whole delivered energy is spent in the failure, straining, and FE.

In view of (1), theoretical evaluation of E_f is very important and necessary, as well as its comparison with the available experimental data. Let us first evaluate E_c. Suppose that E_c is accumulated in some volume $V = l^3$, where l is a linear dimension of the strained area adjacent to the crack front. Taking into account that compressibility is defined as $\beta = -V^{-1}(\partial V/\partial P)_T = 1/K$, where K is the volume elasticity modulus, and $dE_c = -PdV = \beta VPdP$ [17], we obtain

$$E_c = \beta P^2 V/2, \qquad (2)$$

where P is the failure pressure. In [15], it was shown that the cleavage process depends essentially on the solid shape and size (Fig. 1): $x(y'/2)$ is the size along the crack propagation in xz plane; z' and $2y'$ are the width and thickness, respectively. As may be necessary, for further estimations we take $z' = 2y' = x' = 1$ cm.

Some part of energy, $E_s = \gamma s$, is spent [15, 16] to formation of a new surface $s(xz) = 2\delta^2$, where $\gamma(xz) = 3a^2/\pi^2\beta\ (1 - 2\nu)y_0$ is the specific surface energyp; ν, the Poisson coefficient; y_0, the equilibrium interplanar spacing in y direction, and a is the "extinction distance" for the attracting force. $E_d = 9\gamma l^2 \ln[3(1 - 2\nu)/2\pi\sigma_y\beta(1 + \nu)]$ is the plastic strain energy on δ^2 crack surface exposure, where σ_y is the strain at the crack front along y direction; $E_k \approx E_c(v_c/v_s)^2$, where v_c is the crack propagation speed; $v_s = [\rho\beta\ (1 - 2\nu)]^{-0.5}$ is the speed of longitudinal acoustic waves, and ρ is the crystal density.

For numerical evaluations according to (1) and (2), let us consider the most studied process of LiF fracturing, including the experimental data on FE [9, 10] and using the following values given in Table: $\beta = 1/K = 1.43\cdot10^{-12}$ cm^2/dyn and $\nu = 0.217$ [18, 19]; $\gamma(100) = 374$ erg/cm^2 [15]; $v_c = 3.9\cdot10^5$ cm/s [10]; $v_s = 7.143\cdot10^5$ cm/s [18]; $P = 4.73\cdot10^{10}$ dyn/cm^2 [20]. Let us take $P \approx \sigma_{100}$. Assuming $\delta = 10^{-5}$ cm and using (2), we obtain, in erg$\cdot10^7$: $E_c \approx 16$, $E_s \approx 0.374$, $E_d \approx 4$, and $E_k \approx 0.3$, $E_c \approx 5$. From (1), $E_e + E_f \approx 7\cdot10^{-7}$ erg $\approx 4\cdot10^5$ eV. Assume to a first approximation $E_e = 0$ and compare E_f with the dissociation energy of LiF into ions, $LiF \rightarrow Li^+ + F^-$, $u_i = 10.51$ eV [21], or into atoms, $LiF \rightarrow Li + F$, $u_a = 8.83$ eV [10], to estimate roughly the intensity of FE. Calculating $p = E_f/u$ ratio, we obtain the number of Li and F atom pairs, $p_a = E_f/u_a \approx 5\cdot10^4$, or $5\cdot10^{14}$ cm^{-2} emitted from the environment δ of the crack front. The observed experimental value is $p_a \approx I \sim 10^{13}$ atom/cm^2 (in the opinion of the authors [9–11], this value presents the lower limit for LiF, see Table, due to high chemical activity of the atoms with respect to the material of the measuring system).

The calculations (Table) make it possible not only to estimate numerically the channels of energy dissipation at the crack front, but to determine its elastic component E_e, its fraction exceeding a half of the full crack energy E_c, except for NaCl and LiF. The contribution of E_d and E_k energies into (1) is also significant (except for KF and KCl), and $E_d \sim E_k$. The crack energy spent for FE is not significant, according to the experimental data of [10], and is close to the surface energy of crystals: $E_f \sim E_s$. Noteworthy, the accuracy of calculations is defined both by the postulated $P \approx \sigma_y$ equality and the value of failure pressure P depending essentially on the crystal defects (its origin, prehistory of obtaining, purity, nature of admixtures, etc.) [1–3, 8, 14, 15, 20].

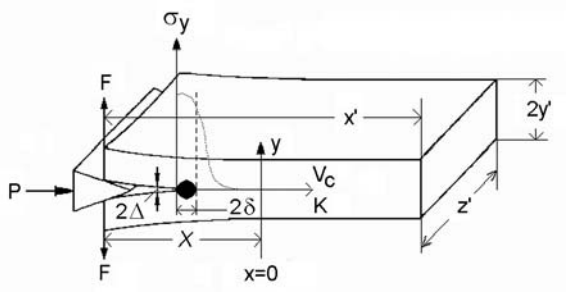

Fig. A sketch of LiF single crystal fracture along the cleavage plane (100) [15].

To evaluate the formation probability of nanoparticles, the emission process of atomic (molecular) aggregates in the cluster unit form has to be considered, too. This process necessitates a single-stage evolution of a significant energy amount in the system, and the best way to the solution of problem is the examination of energy fluctuations therein. So, applying the relationships of statistical mechanics to energy fluctuation ΔE at the crack front, we have analyzed the possibility that some part of E_c was spent in the nanoparticle formation [17].

The following aspects of processes at the crack front are the physical prerequisites for the evaluation of energy fluctuation ΔE. Let us first consider in detail the pre-failure zone (the black area in Figure). This area can be considered as a subsystem in where E_c is accumulated as a result of a stress pulse. The rest fraction of the solid where this energy is absent or at least is significantly less than in the highlighted area can be considered as an environment. Energy E_c referred to the number of bonds in the volume δ^3 can be considered as a small fluctuation if its value is minor in comparison with energy u bounding atoms or ions into a single whole. This is seen from values in Table that ratios $E_c M/A\delta^3\rho u_a$, where $A = 6.02\cdot10^{23}$ is the Avogadro number and M is the molecular

Table. Characteristics of AHC and their cleavage, channels of energy dissipation according to (*1*), (*2*), (*11*), (*12*) and (*13*), sizes and number of nanoparticles being formed at the crack front

Crystal / property	LiF	NaF	KF	NaCl	KCl	Notes
$y_0(100)\cdot10^8$, cm	1.007	1.195	1.530	1.363	1.790	XRD*
γ, erg/cm^2	374	290**	210**	310	318	[15, 16]
$P\cdot10^{-10}$, dyn/cm^2	4.73	5.00	4.12	1.60	2.66	[20]
ν	0.217	0.236	0.274	0.252	0.274	[18]
$\beta\cdot10^{12}$, cm^2/dyn	1.43	2.06	3.13	4.02	5.62	[18]; $\beta = 1/K$
$v_c\cdot10^{-5}$, cm/s	3.9	3.1	2.4	2.4	2.0	[10]
$v_s\cdot10^{-5}$, cm/s	7.14	5.67	4.64	4.54	3.91	[18]
ρ, g/cm^3	2.640	2.804	2.526	2.163	1.988	[18]
$E_c\cdot10^{-5}$, eV	10.0	16.1	16.6	3.21	12.4	$\delta = 10^{-5}$ cm
$(E_e + E_f)\cdot10^{-5}$, eV	4.3	10	12	0.25	8.7	$\delta = 10^{-5}$ cm
u_i, eV (1 eV$\approx$1.6$\cdot10^{-12}$ erg)	10.51	9.297	8.230	7.918	7.189	[21]
u_a, eV	8.83	7.86	7.61	6.65	6.72	[10]
$I\cdot10^{-13}$, atom/cm^2	3.6	2.1	1.1	1.0	0.63	[10]
$(n/L)\cdot10^{-22}$, cm^{-3}	12.26	8.04	5.24	4.46	3.21	[10]
$E_f = B\ v_c\ \delta^2\ n$, eV$\cdot10^{-5}$	0.30	0.16	0.078	0.067	0.040	$\delta = 10^{-5}$ cm
T_m, K	1122	1269	1130	1074	1049	[22]
$\alpha\cdot10^4$, K^{-1}	1.25	1.2	1.0	1.54	1.39	[19, 22]
$(\beta^{-1}\alpha T)\cdot10^{-10}$, dyn/cm^2	2.62	1.7	1.0	1.50	0.742	T = 300 K
$C_V\cdot10^{-6}$, erg/g$\cdot$K^{-1}	16.16	11.15	8.382	8.641	6.909	[22]
$\langle\delta E_2\rangle = (\rho V C_V k)^{0.5}T$	453	389	325	301	258	T = 300 K
eV (at $\delta = 10^{-5}$ cm)	1699	1645	1224	1076	901	$T = T_m$
$\langle\delta E_1\rangle = (\beta^{-1}\alpha T + P)(\beta V k T)^{0.5}$	353	390	360	355	324	T = 300 K
eV (at $\delta = 10^{-5}$ cm)	1350	1470	1070	870	935	$T = T_m$
$\langle\delta E_1\rangle/E_f$ (at T = 300 K)	0.012	0.024	0.046	0.053	0.081	$\delta = 10^{-5}$ cm
$\langle\delta E_1\rangle/E_f$ (at $T = T_m$)	0.045	0.092	0.14	0.13	0.23	$\delta = 10^{-5}$ cm
$R_p\approx y_0(\langle\delta E_1\rangle/u_a)^{0.5}$, nm	0.64	0.84	1.1	1.0	1.2	T = 300 K
(at $\delta = 10^{-5}$ cm $N\approx10^{10}$)		1.2	1.2	1.8	1.6	2.1
R_p ($\delta = 10^{-6}$ cm), nm	0.11	0.15	0.19	0.18	0.22	T = 300 K
($N\approx10^{12}$)	0.22	0.29	0.32	0.28	0.37	$T = T_m$
$R_p(\delta = 10^{-4}$ cm), nm	3.6	4.7	5.9	5.6	7.0	T = 300 K
($N\approx10^8$)	7.0	9.2	10	8.8	12	$T = T_m$
$R_p(\delta = 10^{-3}$ cm), nm	20	27	33	31	39	T = 300 K
($N\approx10^6$)	39	52	57	49	67	$T = T_m$

*) XRD — X-ray diffraction analysis, **) calculated according to this work.

mass of the compound being considered, do not exceed 0.01 even at $u = u_a$ and very small value of $\delta = 10^{-5}$ cm for sufficiently plastic AHC [15, 23]. This allows us to consider the presence of E_c in a subsystem as a small fluctuation. There are two possible ways to consider a system in which small fluctuation is brought. The first way assumes the solution of kinetic equations using methods of irreversible processes

thermodynamics [24]. Another way used by us is based on the Onzager hypothesis according to which the macroscopic non-equilibrium condition near to the equilibrium condition can be considered as a fluctuation. Conditions in a macroscopic non-equilibrium system and in a microscopic system which have undergone the fluctuation vary in time under identical laws. For example, let an inhomogeneous distribution of concentrations and temperatures in a macroscopic system be created. Thus, there will be flows in the system that are described by the appropriate macroscopic laws of transport. If a fluctuation of temperature or concentration occurs in equilibrium system resulting in the same distribution of concentrations and temperatures, then according to Onzager hypothesis, a relaxation of these fluctuations will run under the same laws that control equalization of concentrations or temperatures in a non-equilibrium macroscopic system. As well as during a heat transfer, when there is a transfer of energy from hot (containing excess of energy) to cold areas, a process of energy dissipation from area with energy excess will occur in our case. In this case, during energy change in the "environment — the subsystem" system according to the fluctuation mechanism, the energy allocation process will prevail, and in this sense, the fluctuations are irreversible.

Further, to proof the application legitimacy of equilibrium thermodynamics relationships for system where an emission of particles occurs, it is necessary to find out how much the number of particles and energy in the allocated volume varies as a result of emission. To that end, let us accept the E_c as the system energy, and let us consider the energy fraction which leaves the allocated volume as the size of energy fluctuation ΔE, see the formula (11) lower. Let us accept the ratio $\Delta E/E_c$ as infinitesimal parameter. If $\Delta E/E_c << 1$, it will mean that the energy released from the system as a result of fluctuations is too little in comparison with the system energy and thus, the system can be considered as an equilibrium one. At last, let us consider the number of particles in the allocated volume and compare it with number of the particles leaving the considered volume as a result of energy fluctuation. In this case, $\Delta EM/A\delta^3\rho u_a$ value will be an infinitesimal parameter. If $\Delta EM/A\delta^3\rho u_a << 1$, the processes in this system can be described using approaches of equilibrium thermodynamics where the number of particles is kept. The estimations mentioned below (Table) allow to assert that changes of energy and number of particles resulting from fluctuations are very small, and consequently relations of equilibrium thermodynamics are applicable to the problem being under consideration.

Generally, the energy depends on three thermodynamic parameters: volume V, temperature T, and pressure P. Let us write the total differential of energy fluctuation with V and T as independent variables. To that end, we use the expression for energy fluctuation [17]:

$$\Delta E = \Delta V(\partial E/\partial V)_T + \Delta T(\partial E/\partial T)_V = \\ = \Delta V(\partial E/\partial V)_T + C_V\Delta T, \quad (3)$$

where ΔE is the energy of fluctuation caused by volume and temperature fluctuations ΔV and ΔT, respectively, in the system of volume V at temperature T, and $(\partial E/\partial T)_V = C_V$ by definition, where C_V is the heat capacity at constant volume. Further, we use the expressions for differentials of total energy E and free energy F:

$$dE = TdS - PdV, \quad (4)$$

$$dF = -SdT - PdV \quad \text{or} \quad (\partial F/\partial T)_V = -S \quad (5)$$
$$\text{and} \quad d^2F/dVdT = -(dS/dV)_T.$$

As $dF/dV = -P$, taking the derivatives of F, first with respect to volume and then to temperature, we obtain, using (5), the following expression:

$$d^2F/dTdV = -(dP/dT)_V = -(dS/dV)_T. \quad (6)$$

Then we can substitute in (3), using (4):

$$(\partial E/\partial V)_T = T(dS/dV)_T - P, \quad (7)$$

$$\Delta E = [T(\partial P/\partial T)_V - P] + C_V\Delta T. \quad (8)$$

Note that the average values of fluctuations go to zero, i.e. $<\Delta T> = 0$ and $<\Delta V> = 0$, and in (3), the momentary values of ΔE, ΔV, and ΔT are presented. In the experiments, however, only the average values of physical quantities can be observed. Hence, ΔE has to be squared for averaging. As the fluctuations of temperature and volume are statistically independent, the average value of the product goes to zero, $<\Delta V\Delta T> = 0$. When squaring (8), the cross terms containing $\Delta T\Delta V$ product will go to zero

$$<\Delta E>^2 = [T(\partial P/\partial T)_V - P]^2<\Delta V^2> + \quad (9)$$
$$+ C_V^2<\Delta T^2>.$$

Using the expressions obtained in [17] for the average square values of fluctuations for T (in centigrade), $<\Delta T^2> = kT^2/C_V$, and V, $<\Delta V^2> = -kT(\partial V/\partial P)_T$, we find

$$<\Delta E>^2 = \quad (10)$$
$$= -[T(\partial P/\partial T)_V - P]^2 kT(\partial V/\partial P)_T + C_V kT^2,$$

where $k = 1.38\cdot10^{-16}$ erg·K^{-1} is the Boltzmann constant. Introducing $\beta = -V^{-1}(\partial V/\partial P)_T$ and the coefficient of volume thermal expansion $\alpha = V^{-1}(\partial V/\partial T)_p$, for the specific heat capacity C_V [22], expression (10) for the crack front takes the form

$$<\Delta E>^2 = <\Delta E_1>^2 + <\Delta E_2>^2 = \quad (11)$$
$$= (\beta^{-1}\alpha T + P)^2 \beta VkT + \rho V C_V kT^2.$$

The $C_V kT^2$ term characterizes the value of energy fluctuation for the mass $\rho V = \rho\delta^3$ of the crack front area at thermal equilibrium under temperature T. The expression in brackets represents the contribution of temperature and pressure P to the sought quantity of energy fluctuation. It seems of interest to evaluate not only the values of $<\Delta E_1>$ and $<\Delta E_2>$ items, but also their extreme temperature characteristics. The crystalline state of substance, as well as the temperature pulse at the crack front [23, 25, 26] is limited by the crystal melting temperature T_m. As $P \sim \beta^{-1}\alpha T$ (Table), contributions of the items are nearly equal: $<\Delta E_1> \approx <\Delta E_2>$. The equilibrium constituent of fluctuation energy $<\Delta E_2>$ is spent for lattice vibrations (phonon scattering) within the crystal volume, raising its average temperature by
$<\Delta T> = <\Delta E_2>\delta/y'\rho V C_V = <\Delta E_2>/y'\rho\delta^2 C_V \sim 10^{-6}$ K, if $\delta = 10^{-5}$ cm and $2y' = 1$ cm. So, we consider below only the first item $<\Delta E_1>$ in equation (11) that includes three components of fluctuation energy of the same order (Table), $\beta^{-1}\alpha^2 VkT^3$ (thermic), $2\alpha VPkT^2$ (mixed), and $\beta VP^2 kT$ (mechanic).

Let us compare the values of $<\Delta E_1>$ with the experimental values E_f. Correlation between the crystal parameters and FE intensity I is defined by the expression $I = Bv_c n/uL \approx hv_c n/uL$ [10]. Here, n [cm^{-2}] is the number of broken and/or excited bonds at the failure surface, $L \approx y_0$ [cm] is the typical chemical bond length in the crystal [10], u [erg/molecule (atom)] is the energy of solitary FE, and $B = 10^{-26}$ erg/s is an empirical parameter of the correlation, close (equal [12]) to the Planck constant $h = 6.63\cdot10^{-27}$ erg/s. If we assume $u = u_a$, then the product Iu on the open failure surface, $(V)^{2/3} = \delta^2$, gives the measured energy E_f:

$$E_f = Bv_c\delta^2 n/L \approx hv_c\delta^2 n/L. \quad (12)$$

The analysis of the (11) to (12) ratio gives the information about the FE mechanism:

$$<\Delta E_1>/E_f \approx \quad (13)$$
$$\approx (\beta^{-1}\alpha T + P)(\beta kT/\delta)^{0.5}[Bv_c(n/L)]^{-1}.$$

If $<\Delta E_1>/E_f >> 1$, the energy fluctuations are significant, and only some fraction thereof is realized as FE. The remaining fraction is dispersed through the other energy dissipation channels. When $<\Delta E_1>/E_f \approx 1$, the fluctuation energy is mainly spent for FE, and if $<\Delta E_1>/E_f << 1$, the energy fluctuations are small and only some fraction of the full intensity of FE or a certain kind of FE may be realized via the fluctuation mechanism. Calculations (Table) showed that, at any temperature T acceptable for the crystal, the last variant occurs, and as the interplanar spacing (ion size) increases, the fluctuation energy rises, whereas the FE intensities fall monotonously.

The release of $<\Delta E_1>$ energy in volume V is insufficient for the elementary act of AHC sublimation. Hence, it is reasonable to use it to estimate the parameters of nanoparticle emission at the crack front. When the atoms are arranged in a cluster, the bond energy is gained, and if the amount of the bonds is sufficient, the fluctuation energy becomes sufficient for the emission of a particle from the crystal lattice, the particle containing some pairs of atoms p with a radius R_p. Calculations for AHC given in Table represent the range of $\delta = 10^{-3} \div 10^{-6}$ cm and admit equal bond energies in crystal and cluster.

The calculations were carried out taking LiF as an example, assuming $\delta = 10^{-5}$ and $T = 300$ K. To break one bond, energy ua is necessary, and the failure surface $s_a \approx \pi(y_0/2)^2$ appears in a crystal. If we admit that all $<\Delta E_1>$ energy is spent for the bond breaking, the cluster surface will be $s_p<\Delta E_1> s_a/u_a \approx 4\pi R_p^2$. Hence, $R_p \approx y_0(<\Delta E_1>/u_a)^{0.5} \approx 0.64$ nm, and the num-

ber N of such particles at the fracture of a real crystal (Fig. 1) will be $N \approx x'z'/\delta^2 \approx 10^{10}$, that is, about three orders less than the number of neutral atoms emitted from the crack front.

As $<\Delta E_1> \sim \delta^{1.5}$, it is easy, using the data of Table 1, to find the dimensions of clusters for δ values different from $\delta = 10^{-5}$ cm: $R_p(\delta) \approx R_p(\delta = 10^{-5}\ \text{cm}) \cdot (\delta/10^{-5}\ \text{cm})^{0.75}$. The last and obligatory comment to Table 1 should attract attention to the fact that both the diameter ($2R_p = 0.2$ to 130 nm) and the number of clusters ($N = 10^{12}$ to 10^6) are functions of linear dimension δ of the strained area at the crack front during the process of AHC failure. The δ value is difficult to evaluate correctly using both theoretical and/or practical means. Therefore, a simultaneous experimental measuring of R_p and N at AHC cleavage could advance a new method for the evaluation. For example, dual-frequency coherent-optical method [27], mass-spectrometry [11], or electron microscopy methods [28] could be applied.

To conclude it is to note that the methods of quantum theory [29] and discrete lattices [30] were engaged in the analysis of the phenomena at the crack front, but FE was not considered. The FE evaluation carried out in this work shows that, in spite of its insignificant contribution to the total energy balance of the dynamics of solid failure, it not only completes the set of phenomena and processes at the crack front, but also can provide a new method for the study of a specific strained area at the crack front. The problem of subnano- [11] and nanoparticles [13] emission at the crack front is discussed for the first time. We predict the possibility of this process basing on the following considerations: a) large enough values of P and T in some environment δ of the crack front; b) according to the laws of statistical physics [17], dynamic variation of P and T results in an energy fluctuation in the volume δ^3; c) the analysis of a single-step release of fluctuation energy shows that it is comparable with the energy of nanocrystal particle formation at the crack front.

This work was partially financially supported by the Integration grant of the SB RAS and Russian Foundation for Basic Research (03-03-32271 and 05-05-64572).

References

1. J.E.Field, *Contemporary Physics*, **12**, 1 (1971).
2. G.P.Cherepanov, Mechanics of Brittle Fracture, Nauka, Moscow (1974) [in Russian].
3. V.R.Regel', A.I.Slutsker, E.E.Tomashevskii, Kinetic Nature of the Strength of Solids, Nauka, Moscow (1974) [in Russian].
4. F.Kh.Urakaev, V.V.Boldyrev, *Russian J. Phys. Chem.*, **74**, 1334 (2000).
5. C.Suryanarayana, *Progr. Mater. Sci.*, **46**, 1 (2001).
6. G.Heinicke, Tribochemistry, Akadem.-Verl., Berlin (1984).
7. J.T.Dickinson, in: Non-Destructive Testing of Fibre-Reinforced Plastics Composites, ed. by J.Summerscales, Elsevier, L.-N. Y. (1990), v.2, p.429.
8. V.A.Zakrevskii, A.V.Shuldiner, *Phil. Mag.*, **B71**, 127 (1995).
9. T.E.Gallon, J.H.Higginbotham, M.Prutton, H.Tokutaka, *Surface Sci.*, **21**, 224 (1970).
10. F.Kh.Urakaev, V.V.Boldyrev, *Russian J. Phys. Chem.*, **74**, 1339 (2000).
11. J.T.Dickinson, L.C.Jensen, S.C.Langford, *Phys. Rev. Lett.*, **66**, 2120 (1991).
12. F.Kh.Urakaev, I.A.Massalimov, *Mendeleev Communications*, **13**, 172 (2003).
13. O.F.Pozdnjakov, B.P.Redkov, in: Abstr. of VIII All-Union Symp. on Mechanoemission Mechanochemistry of Solids, USSR Acad. Sci. Publ., Tallinn (1990), p.86 [in Russian].
14. H.Rumpf, Symposion Zerkleinern, Verlag Chemie GMBH, Vienna (1962), p.7.
15. J.J.Gilman, in: Fracture, John Wiley and Sons, New York-London (1956), p.217.
16. R.Shuttleworth, *Proc. Phys. Soc. London*, **A62**, 167 (1949).
17. L.D.Landau, E.M.Lifshits, Statistical Physics, Pergamon Press, Oxford (1980), p.35,334.
18. O.L.Anderson, in: Lattice Dynamics, ed. by W.P.Mason, Ac. Press, New York (1965), p.62.
19. Handbook of Physical Constants, ed. by S.P.Clark, Jr., Geol. Soc. Am., Connecticut (1966).
20. N.McMillan, in: Atomistic of Fracture, ed. by R.M.Latanison and J.R.Pickens, Plenum Press, New York (1983), p.28.
21. Ch.Kittel, Introduction to Solid State Physics, John Wiley and Sons Inc., New York (1975).
22. Tables of Physical Values, ed. by I.K. Kikoin, Atomizdat, Moscow (1976) [in Russian].
23. M.I.Molotskii, *Sov. Sci. Rev. Series, Sect. B:Chem. Rev.*, **13**, 1 (1989).
24. R.Kubo, *J. Phys. Soc. Japan*, **12**, 570 (1957).
25. F.P.Bowden, P.A.Persson, *Proc. Roy. Soc. London*, **A260**, 433 (1961).
26. F.Kh.Urakaev, V.V.Boldyrev, *Powder Technology*, **107**, 197 (2000).
27. F.Kh.Urakaev, L.Sh.Bazarov, I.N.Meshcheryakov et al., *J. Cryst. Growth*, **205**, 223 (1999).
28. S.C.Langford, M.Zhenyi, L.C.Jensen et al., *J. Vac. Sci. Technol.*, **A8**, 3470 (1990).

29. R.Thomson, in: Atomistic of Fracture, ed. by R.M.Latanison and J.R.Pickens, Plenum Press, New York (1983), p.167.

30. J.F.Knott, in: Atomistic of Fracture, ed. by R.M.Latanison and J.R.Pickens, Plenum Press, New York (1983), p.209.

Емісія наночастинок на фронті тріщини при розколюванні лужно-галоїдних монокристалів

І.А.Массалімов, І.А.Мадюков, В.С.Шевченко, Ф.Х.Уракаєв

Рівняння статистичної фізики застосовано до числових аспектів енергетичного балансу при фронті тріщини для випадку розколювання лужно-галоїдних монокристалів. Теоретично оцінено ймовірність утворення наночастинок у процесі динамічного руйнування.